SCA2003-50

MAPPING FRACTURE APERTURES USING MICRO COMPUTED TOMOGRAPHY

Z. Karpyn, A. Alajmi, C. Parada, A. S. Grader, P.M. Halleck, and O. Karacan.
The Pennsylvania State University

ABSTRACT

Multi-phase flow in fractures plays a significant role during hydrocarbon recovery processes as well as in contaminant transport. With the advent of high-resolution Micro Computed Tomography it is possible in some cases to acquire three-dimensional fracture structures and to determine fracture aperture maps. This paper highlights several examples where artificially created fractures were imaged and the distributions of fracture apertures were determined. The fracture apertures were up to about 1000 microns (1mm) and as low as 50 microns (0.05mm). The spatial pixel resolution was between 20 and 50 microns. At this high-resolution, hundreds and even thousands of two-dimensional slices form the three-dimensional digital core. The fracture is extracted numerically by various processes such as thresh-holding, dilation, and erosion. The extracted aperture maps quantify the topology of the fracture surfaces as well as to the various scales of aperture behavior. In the case of a layered Berea we were able to show some relationship between high permeability layers and high fracture aperture, thus confirming some fluid flow observations. The fracture aperture maps can be used as the basis for multi-phase simulation of fracture transport.

INTRODUCTION

Computed Tomography is a non-destructive imaging technique that uses X-rays and mathematical reconstruction algorithms to view cross-sectional slices through an object. Hounsfield, 1979 Nobel Prize winner in Medicine, developed the first CT-imaging technique in Great Britain in 1972 and was primarily used for medical purposes. Computed Tomography has been used to visualize rock heterogeneities and the determination of lithologies, fluid saturations, porosities, densities and mean atomic numbers, and the visualization of miscible and immiscible flow in rock samples. The determination of fracture topology poses significant challenges. Walters et al. (1998) [1] presented a method for extracting fracture aperture from CT data with voxel sizes similar to ones obtained by medical scanners. However, medical scanners lack in the ability to accurately resolve fractures topologies. MicroCT imaging may provide details of fracture topology but can only view relatively small samples sizes. Alajmi and Grader (2000) [2] and Grader *et al.* (2000) [3] studied fracture-matrix flow interactions in layered Berea samples. Temporal and spatial saturation distributions were determined using X-ray CT in two different flow scenarios: diverging flow from the fracture into the matrix, and converging flow back into the fracture. Porosity in the fractured zone was also correlated with fracture aperture using CT. In the present paper, several artificially created fractures were studied through visualization and quantification using Computed Tomography (CT). Findings of Alajmi and Grader (2000) and Grader *et al.* (2000) were confirmed. The superiority of the high-resolution images over the corresponding low-resolution medical

scans is presented. The methodology developed contributes to the correlation of multi-phase fluid conductivities with fracture geometry and topology and can be used for a variety of fluid flow simulations.

EXPERIMENTS AND METHOD

The rock samples were layered Berea sandstones with about 5% clay content, and porosities ranging between 18-22%. Core diameters were ranged between 25 and 50 mm, and lengths varied from 100 to 380 mm. Samples were cored parallel to the bedding planes. The induced fracture is perpendicular to the bedding in sample 1, and parallel to bedding in samples 2 and 3. Core samples were fractured by a Brazilian-like test. In order to obtain a longitudinal fracture, the cylindrical sample was compressed between two parallel plates with a diameter of 150 mm, thereby inducing a tensile state of stress in the center of the cylinder. As the compression of the core is increased, a fracture is formed along the longitudinal direction of the core. The experimental installation used in these experiments includes a multi-phase fluid flow system, a core holder assembly, and an X-ray Computed Tomography system. Two CT units were used: a medical system, HD250, and an industrial system, OMNI-X. Typical resolutions used in this paper were: HD250 - 0.25x0.25x2 mm, OMNI-X- 0.02-0.05 mm. Through a numerical process that includes thresh-holding, erosion and dilation, a two-dimensional map of aperture distribution is extracted from the data set. The distance between the two fracture surfaces is measured and projected onto a common plane. The resulting two-dimensional aperture map has a length that was scanned, and its width is the diameter of the core.

RESULTS AND DISCUSSION

A qualitative comparison of CT imaging capabilities is presented in **Figure 1**. This figure displays on the left an image acquired with the medical scanner and its high-resolution version on the right side. Due to the resolution of the medical scanner, the matrix shows smooth layers of different rock densities, and just a few incrustations or heterogeneities. The fracture appears to be open at the edge and continuous, and it is well differentiated from the matrix. Each pixel in the first image represents a rock volume of 0.25x0.25x2.0 mm. In addition, the resolution of the medical scanner and the large density contrast between the fracture and the matrix create the appearance of a large fracture width, which is resolved in the high-resolution images of the OMNI-X scanner, shown on the right. The layering in the high-resolution image is detailed and individual high-density inclusions are visible.

A longitudinal reconstruction of the fracture is presented in **Figure 2**. The length scanned was 38 mm along the main axis of the cylindrical core. The image on the left was generated using 19 individual slices originated from the medical scanner. The same region was scanned with the high-resolution scanner, with about 400 slices shown on the right. The high-resolution scanner was able to capture minute details and heterogeneities in the core. The section acquired by the HD250 appears diffused and shows an overestimated fracture width. The thickness of each image taken by the HD250 is 2 mm,

compared to 0.095 mm on the high-resolution OMNI-X. Due to this difference, the OMNI-X images were stacked in groups of 21 in order to obtain average images with a thickness of 2 mm, equivalent to those obtained by the medical scanner. The stacked high-resolution slices were of superior quality when compared to the medical slices.

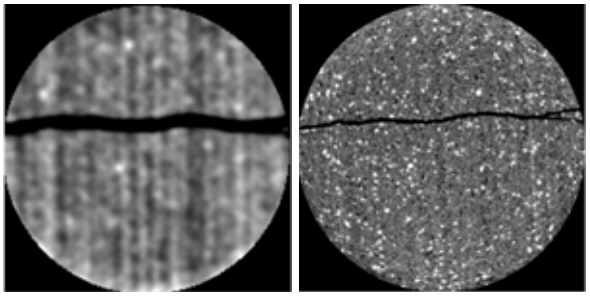

512 x 512 - HD250 1024 x 1024 - OMNI-X

Figure 1: Medical vs. MCT images.

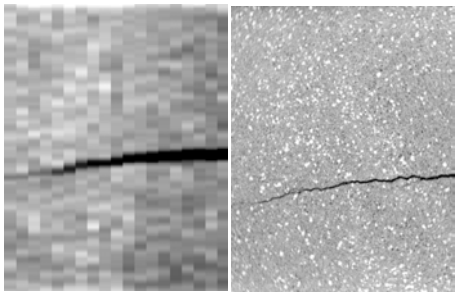

19 images – HD250 400 images – OMNI-X

Figure 2: Medical vs. MCT axials.

Various CT profiles in the induced fracture and its surrounding matrix were also studied. **Figure 3** presents a comparison of these profiles. The averaged CT values reported in the fracture profile represent transverse CT averages measured inside the fracture gap. It is important to avoid boundary effects caused by the surrounding rock matrix or beam hardening. CT profiles taken in the matrix region were located 6 pixels above and below the fracture surfaces. Both profiles show similar trends along the diameter of the core. The presence of heterogeneities and the slightly slanting layers cause mismatches of some peaks. This effect is more notable in the center of the core where the layers are not clearly delineated. Some of the locations where peaks in the matrix and the fracture profiles match are marked by the black vertical lines. There are locations along the profiles where this match is not present. In general, there is a correlation between porosity in the fractured region and the porosity of the adjacent layers. This characteristic was also referred by Alajmi and Grader (2000), and Grader *et al*. (2000).

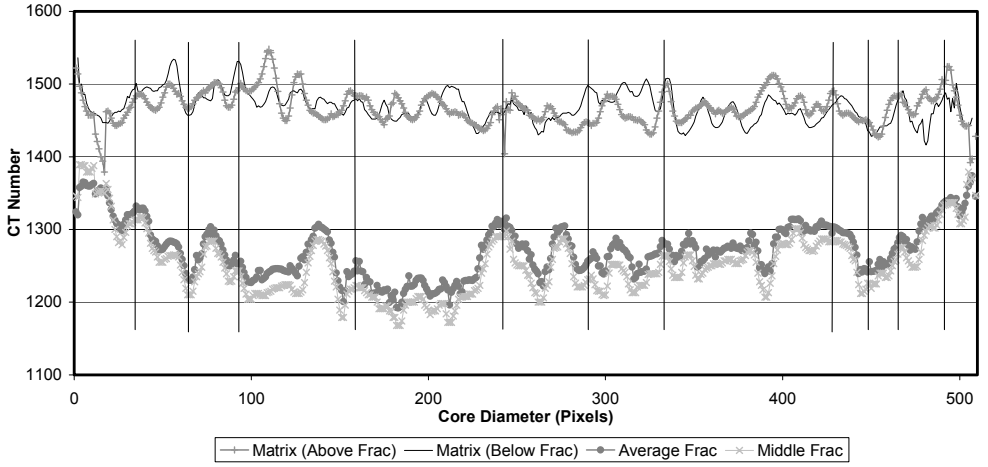

Figure 3: CT profiles in the fracture and the adjoining matrix. OMNI-X.

Two-dimensional aperture maps and three-dimensional topography views were constructed from x-ray MCT data. **Figure 4** (left) shows a typical section of an image obtained with the high-resolution MCT scanner. Each pixel is classified as being part of the pore space or the rock (right). A threshold CT number differentiates the two groups. **Figure 5** shows an expanded detail of a rock sample and a schematic of the procedure used to construct the two-dimensional fracture aperture map. The distance between the two fracture surfaces is measured and projected onto a common plane. This measurement is collected for every slice, thus forming a two-dimensional map. **Figures 6,** and **7** are aperture maps of samples 1, 2, and 3, respectively. The longer side on the map represents the length of the scanned sections in the samples 2 and 3, while the shorter side is the core diameter. White and light grey regions are of larger fracture width, up to a maximum of about 1 mm. Areas in dark grey have smaller widths, in some cases the two fracture surfaces are in contact and form asperities (width=0 mm). The top image in Figure 6 shows an aperture map of a fracture that is perpendicular to bedding. The bedding planes, shown as a CT section at the bottom of Figure 6, are "reflected" in the fracture aperture map. The fracture aperture is large when the fracture intersects a high porosity layer, thus confirming fluid flow observations. This type of analysis permits the computation of fracture volume, as well as demonstration of fracture topology. Further stages in this project include identification of fluid distributions in multi-phase systems and its relation to fracture aperture variations. A three-dimensional view of the fracture body also provides means to characterize the complex structure of a fracture. **Figure 8** presents a three-dimensional view of the fracture volume in sample 3. The black areas are asperities or regions where upper and lower fracture surfaces are in contact. This three-dimensional fracture could be used in a variety of fluid flow simulations, capturing the tortuosity and roughness existent in real fractures.

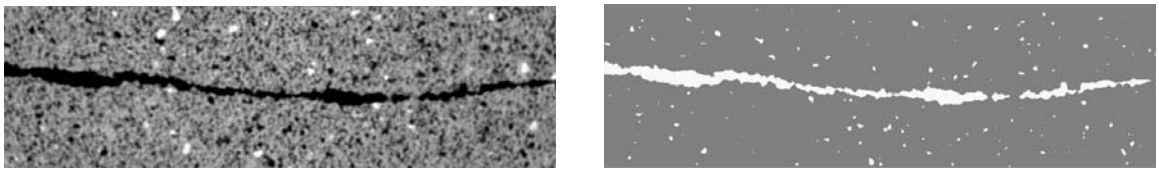

Figure 4: Example of fracture extraction. Left: Original. Right: Partitioned .

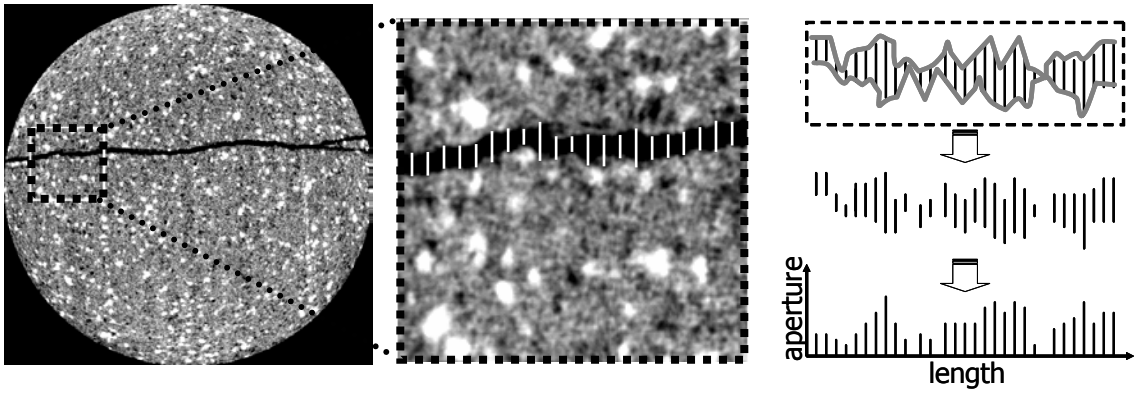

Figure 5: Construction of aperture map from a sample slice.

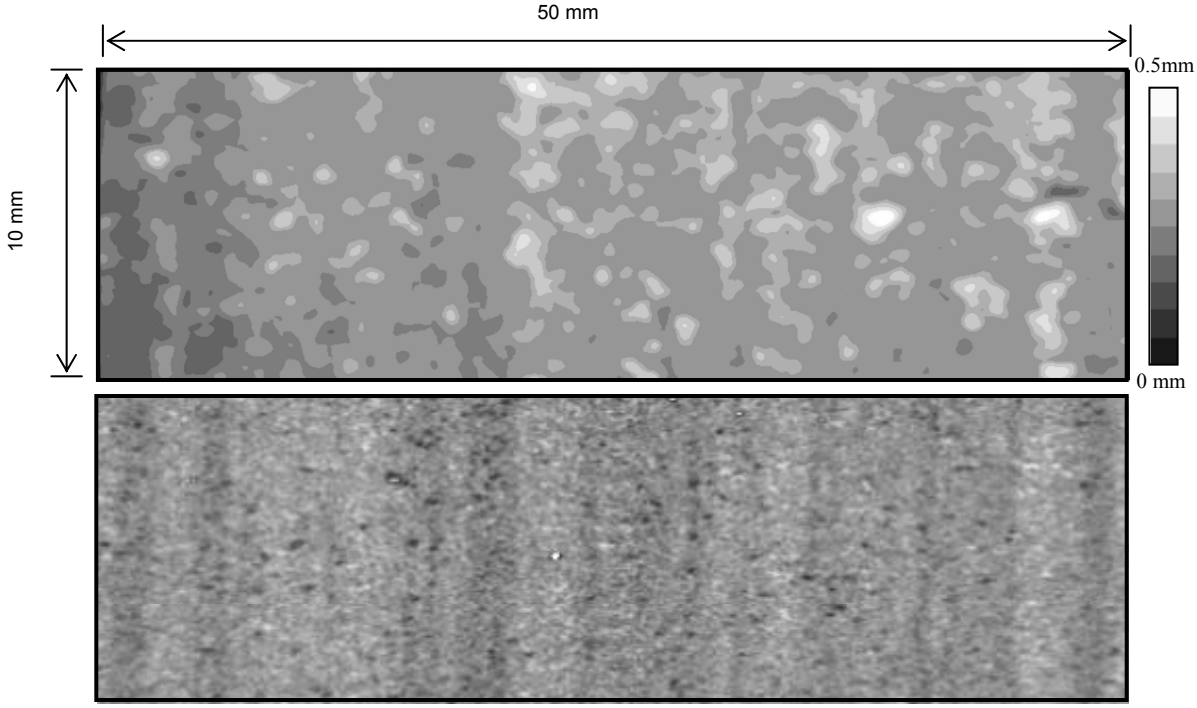

Figure 6: Top: Two-dimensional aperture map in layered sample 1.
Bottom: CT slice of the matrix just below the fracture.

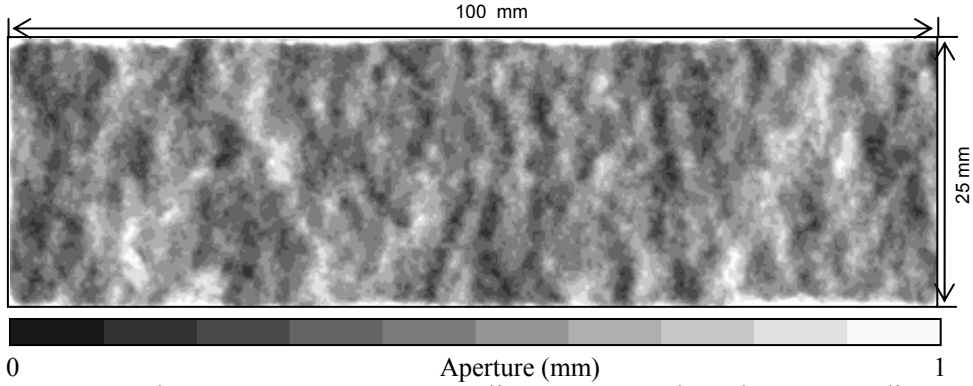

Figure 7: Sample 3 aperture map. 3116 slices, 100 mm long by 25 mm diameter.

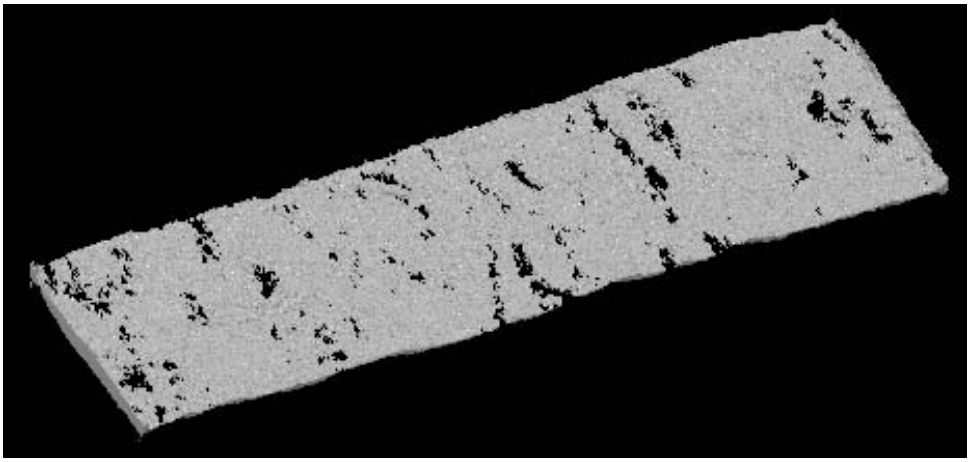

Figure 8: Three-dimensional view of the fracture shown in Figure 8. The black regions are the contact asperities in the fracture. Sample 3.

CONCLUSIONS

- The superiority of the high-resolution images over the corresponding low-resolution medical images was verified.
- A correlation between fracture width and permeability of adjacent rock was observed. Larger fracture apertures correspond to layers of higher permeability in the matrix.
- High-resolution Computed Tomography has proven possible to reconstruct a virtual three-dimensional fracture that can be used for a variety of numerical simulations.
- The methodology developed provided a two-dimensional aperture map of good accuracy, which can contribute to correlation of multi-phase fluid conductivity with fracture geometry and wettability.

ACKNOWLEDGEMETS

The authors acknowledge the supprot of DOE project DE-PS26-01NT41048, the DOE NETL/University Student Partnership Program, The Energy Institute, and the Pennsylvania State University.

REFERENCES

1. Walters, D., Wong, R. and Kantzas, A., "The Application of Computer Assisted Tomography in the Analysis of Fracture Geometry", Geotechnical Testing Journal, GTJODJ, 21(4), 328-335, December 1998.
2. Alajmi, A. F., and Grader, A. S., "Analysis of Fracture-Matrix Fluid Flow Interactions Using X-Ray CT," SPE 65682, Proceedings, SPE Eastern Regional Meeting, Morgantown, West Virginia, 2000.
3. Grader, A. S., Balzarini, M., Radaelli, F., Capasso, G., and Pellegrino, A., "Fracture-Matrix Flow: Quantification and Visualization Using X-ray Computed Tomography," American Geophysical Union Monograph, vol 122, p.1-20, 2000.